



Isolation Characteristics of Silicon Sensors Using Simulation Approach

Kirti Ranjan*, Ashutosh Bhardwaj, Ranjeet Singh, Ram K. Shivpuri

Center for Detector & Related Software Technology (CDRST)

Department of Physics and Astrophysics,

University of Delhi (DU), Delhi, INDIA

RD50 Workshop, Bari, Italy

30 May – 01 June, 2012



Overview

○ Isolation in Si sensors

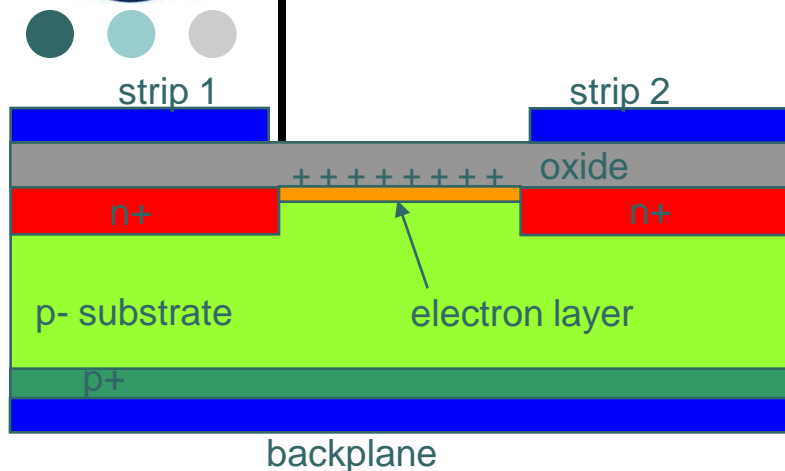
- ✓ R&D for the development of the double sided $p^+-n^-n^+$ Si detectors (DSSDs) for the proposed SiD detector.
- ✓ The designs simulated in the present study are under fabrication at Bharat Electronics Limited (BEL), Bengaluru, India (same place which fabricated CMS Preshowe sensors)
- ✓ **Layout/Geometry**
- ✓ **Results**

○ Double peak electric field profile simulation as part of the RD50 first simulation task

○ Summary



Isolation in Si sensors

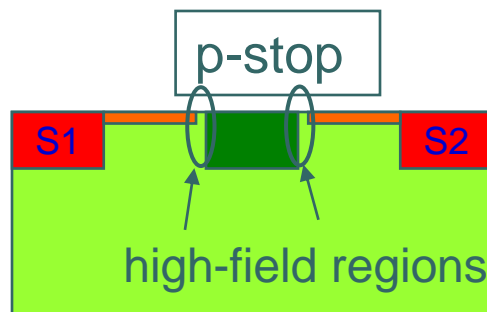
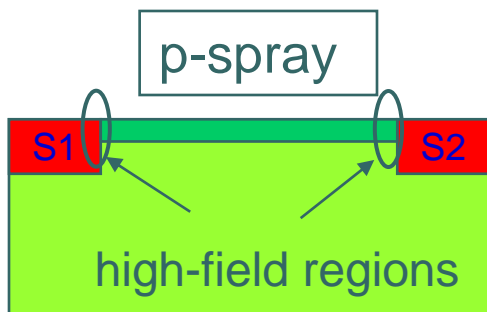


❑ Positive surface charge density (both fabrication and radiation induced).

❑ Shortening due to e- conduction layer in the n^+n^- (or n^+p^- sensors)

- uniform spreading of signal over n^+ strips.
- degradation of position resolution.

❑ Techniques to improve isolation (break conduction channel): P-spray & P-stop



❑ P-spray & P-stop also affect Interstrip Capacitance (C_{int}) & Breakdown voltage (V_{BD}).

Optimized electrical characteristics of the n^+n^- sensors using 2-D TCAD simulation tool – ATLAS (Silvaco, not to confuse with the LHC expt.!) for following techniques: (a) combination of P-spray & P-stop; (b) multiple p-stops & (c) metal overhang over p-stops.

Performance parameters : Interstrip Conductance (G_{int}), C_{int} and V_{BD}



Cross-validation

- ❑ Compared our results with the earlier work “*Device Simulations of Isolation Techniques for Silicon Microstrip Detectors Made on p-Type Substrates*” by Claudio Piemonte, IEEE TRANS. NUCL. SCI., VOL. 53, NO. 3, JUNE 2006. General Trends are same. Validation with some other papers on capacitance and breakdown are also carried out.
- ❑ Working on CMS (Experiment of the LHC) and compared MSSD interstrip capacitance with Simulation => trends are similar (work is ongoing)

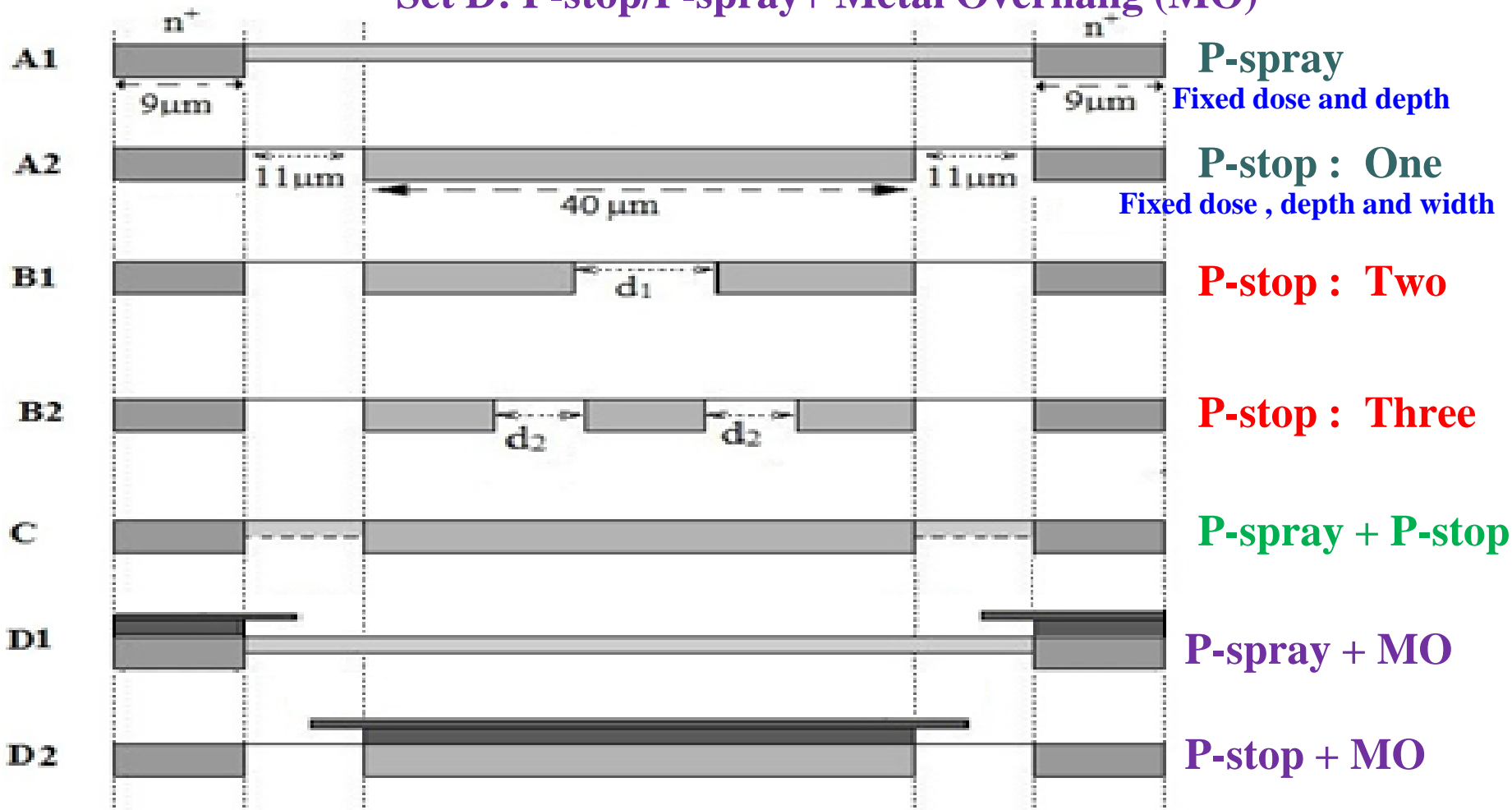


Layout / Geometry

Set B: Multiple P-stops

Set C: P-stop + P-spray

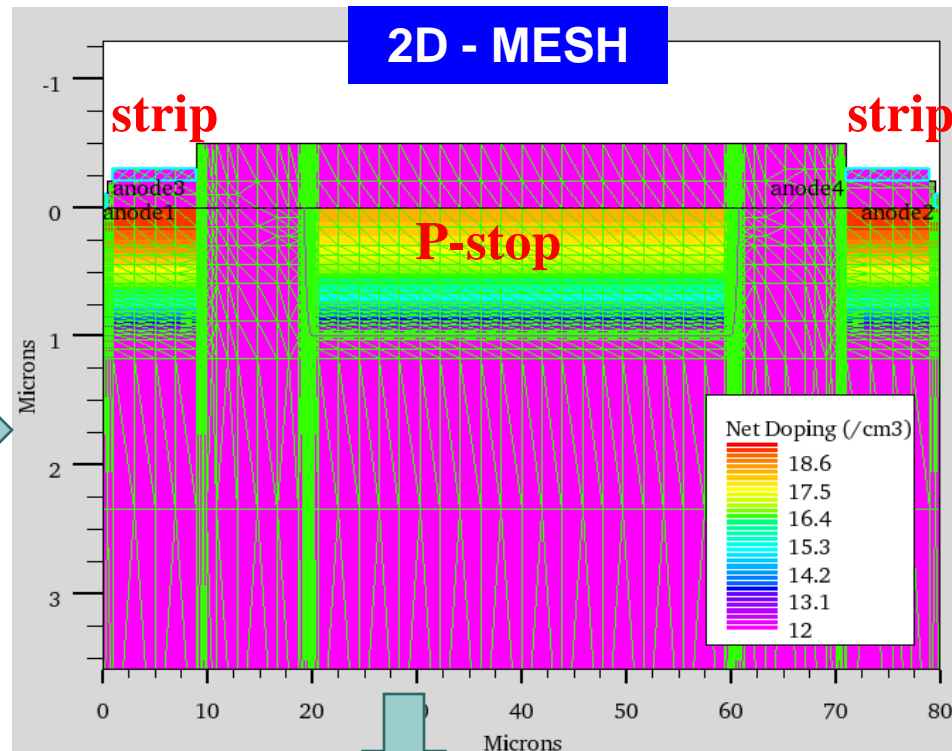
Set D: P-stop/P-spray+ Metal Overhang (MO)





Layout / Geometry

Device Cross-section	300 x 80 μm^2
Junction depth (X_j)	1 μm
Strip pitch	80 μm
Strip width	18 μm
n^+ conc.	$1 \times 10^{19} \text{ cm}^{-3}$
n- Substrate conc.	$7 \times 10^{11} \text{ cm}^{-3}$
Peak p-spray conc.	$2.8 \times 10^{17} \text{ cm}^{-3}$
P-spray depth	0.5 μm
Peak p-stop conc.	$1 \times 10^{18} \text{ cm}^{-3}$
P-stop depth	1 μm
P-stop width	40 μm
Positive oxide charge density (Q_F)	Non-irrad: $1 \times 10^{11} \text{ cm}^{-2}$
	Irrad: up to $3 \times 10^{12} \text{ cm}^{-2}$



Boundary Conditions (BC)

Ohmic BC: Implemented as Dirichlet BC.

Current BC: The floating contacts are implemented using current BC.

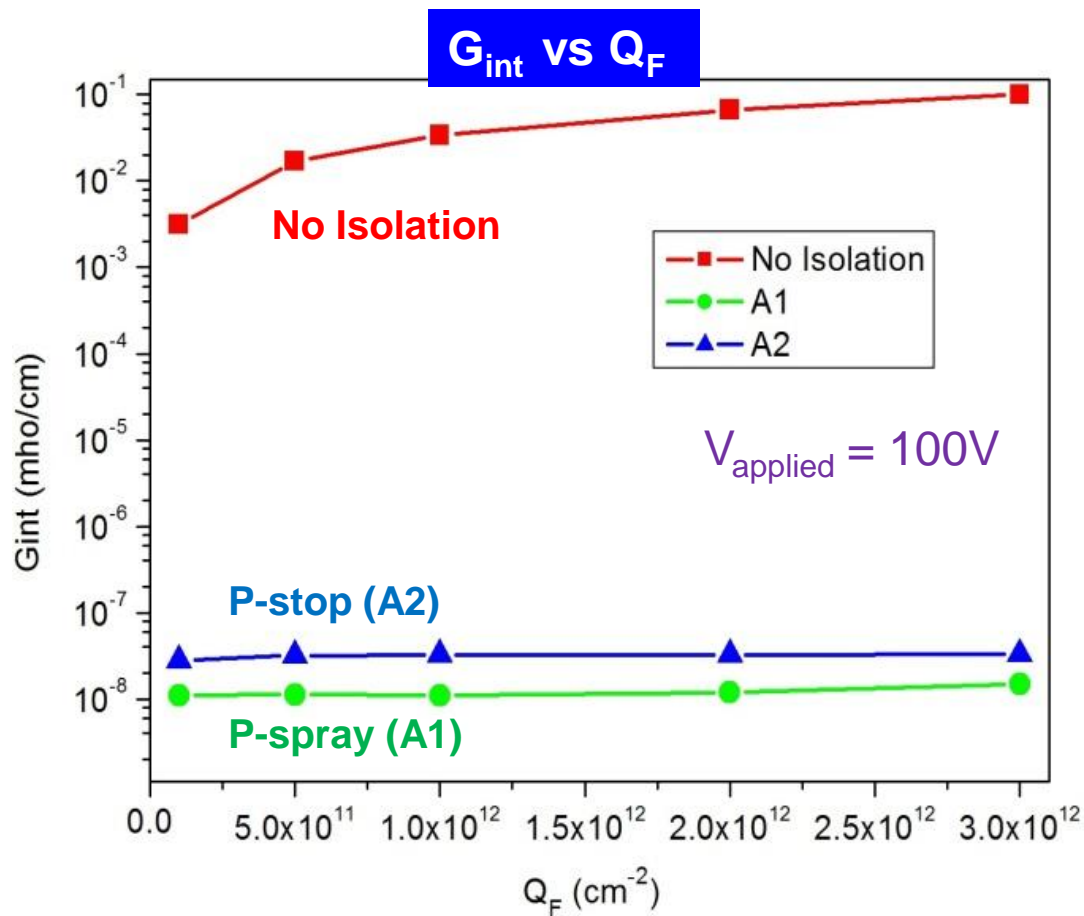
Neumann BC: Along the outer (non contact) edges of devices, homogeneous (reflecting) Neumann BC are imposed so that current only flows out of the device through the contacts.

AC small signal analysis: performed as a post-processing operation to a DC solution. The results of AC simulations are the conductance and capacitance between each pair of electrodes @ f=1 MHz.





Set A: P-Spray and P-stop

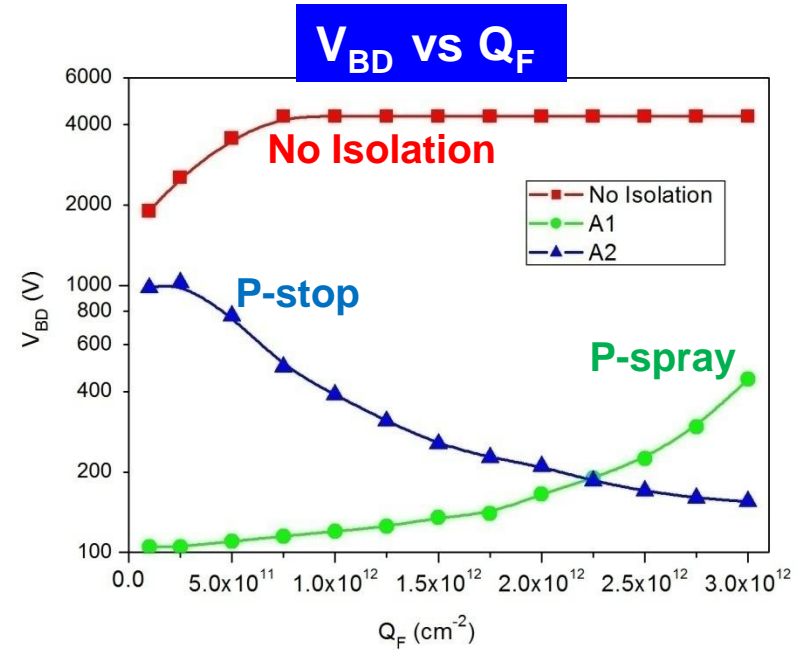
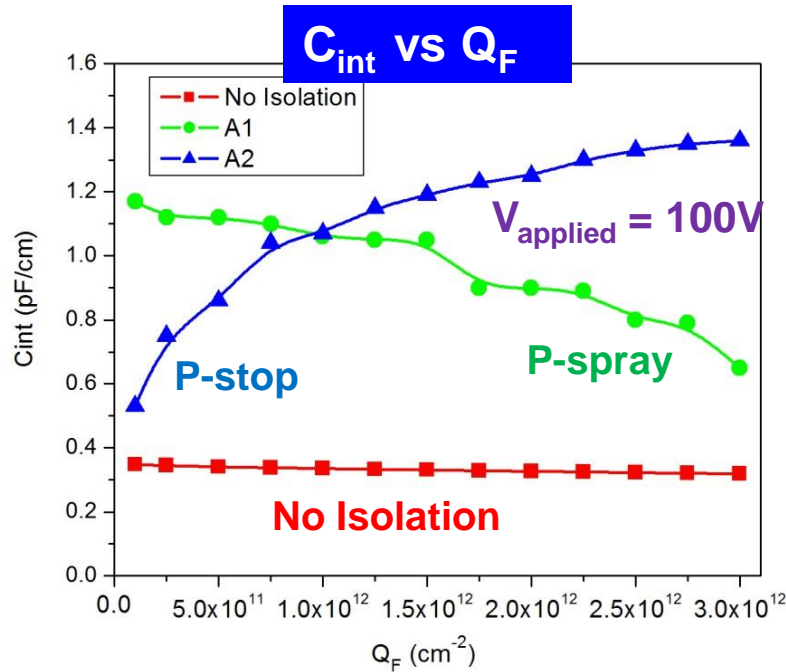


✓ Sensor having no isolation structure has large G_{int} (indicating poor isolation) even at the low values of Q_F

✓ A1 (p-spray) and A2 (p-stop) with the chosen parameters provide isolation at all values of Q_F



Set A: P-Spray and P-stop



For No isolation structure: G_{int} 😞 C_{int} 😊 V_{BD} 😊

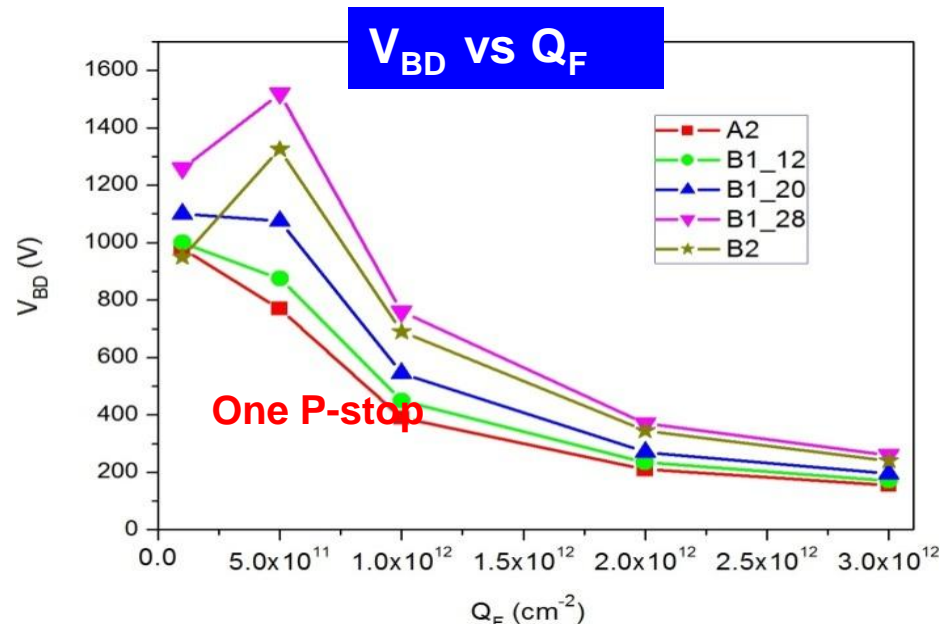
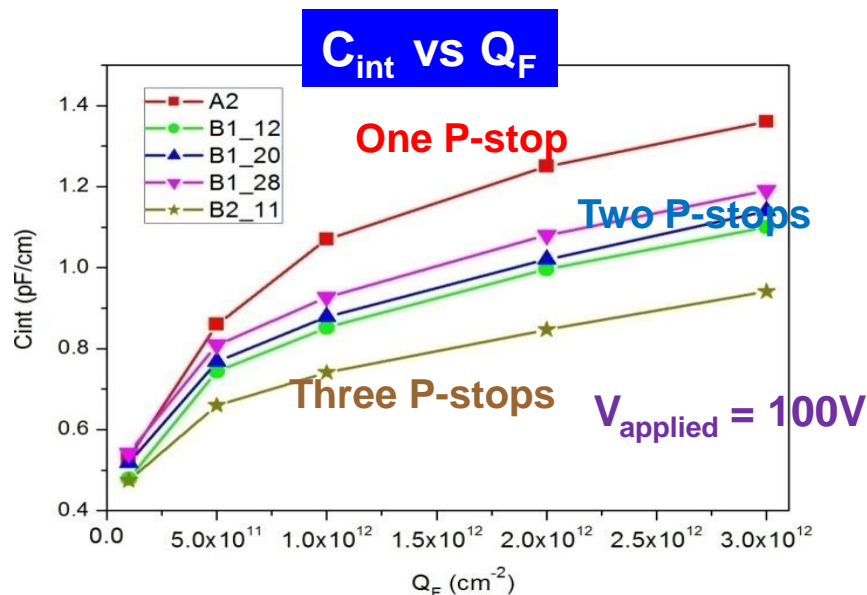
- For P-spray, C_{int} is high & V_{BD} is low for small Q_F & improve w/ increase in Q_F .
- For P-stop, C_{int} is low & V_{BD} is high for small Q_F & deteriorate w/ increase in Q_F .

C_{int} and V_{BD} degrade for both as compared to a structure without isolation. Investigate sensors equipped with isolation techniques, which, while ensuring isolation at all Q_F , should ensure better performance of V_{BD} and C_{int} .



Set B: Multiple P-stops

- 3 configurations of **two p-stops** (B1) w/ different gap (12, 20 & 28 μm)
- 1 configuration of the **three p-stops** (B2) w/ gap = 11 μm .



- C_{int} : An increase in Q_F results in an increase in the C_{int} .
Single p-stop (A2) has highest C_{int} & B2 with triple p-stops has lowest C_{int} .
- V_{BD} : Single p-stop has lowest V_{BD} .
For B1, wider p-stop (B1_12) has lower V_{BD} than narrower p-stop (B1_28).
 V_{BD} of the triple p-stop (B2) is almost same as that of B1_28.

Triple p-stop structure gives better parameter values under investigation.



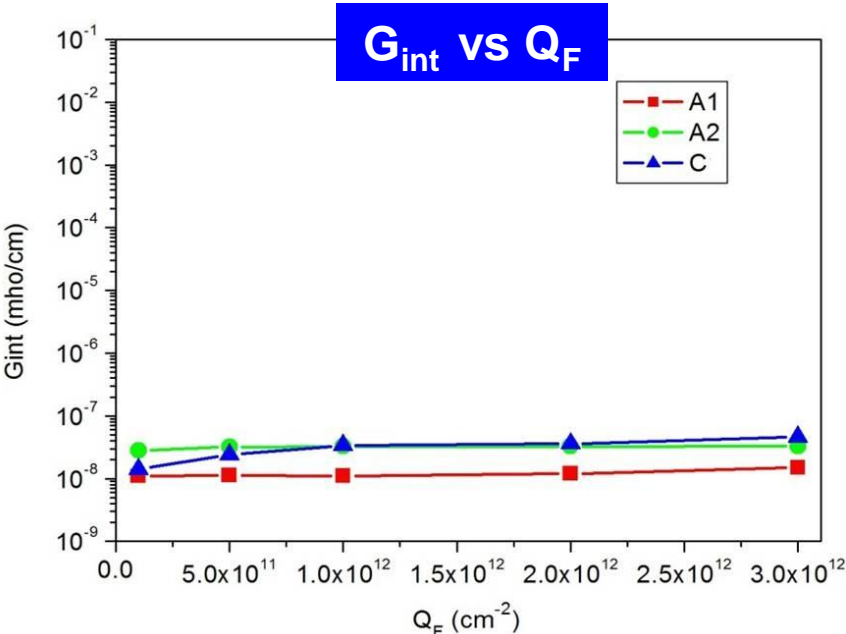
Set C: P-spray + P-stop

Simulation was performed for various values of the peak doping conc. of the p-spray (N_{pspray}) and p-stop (N_{pstop}).

Results vary between two extremes such that in one case p-spray guides the result and in another p-stop.

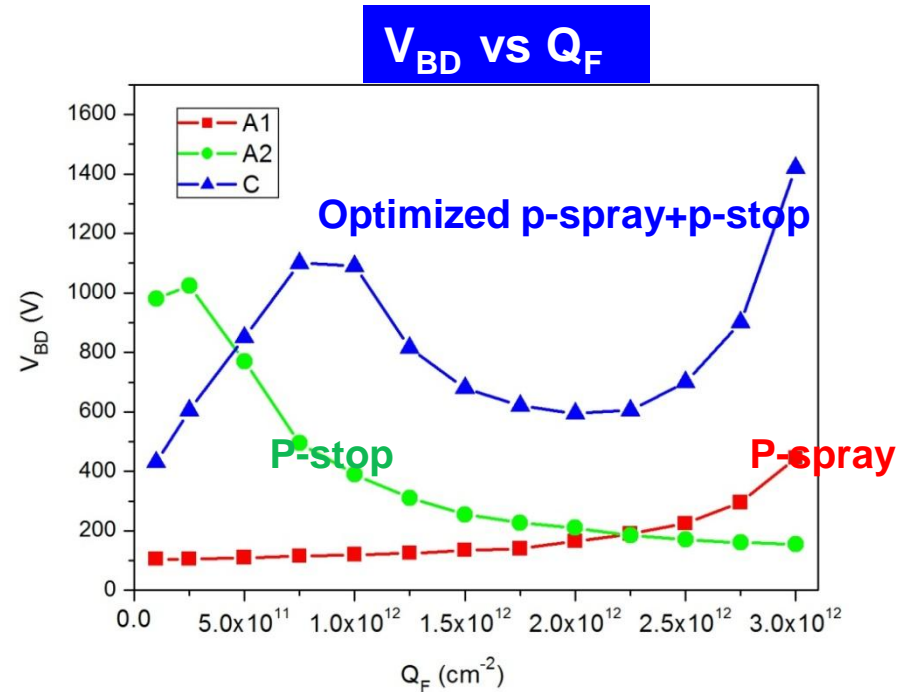
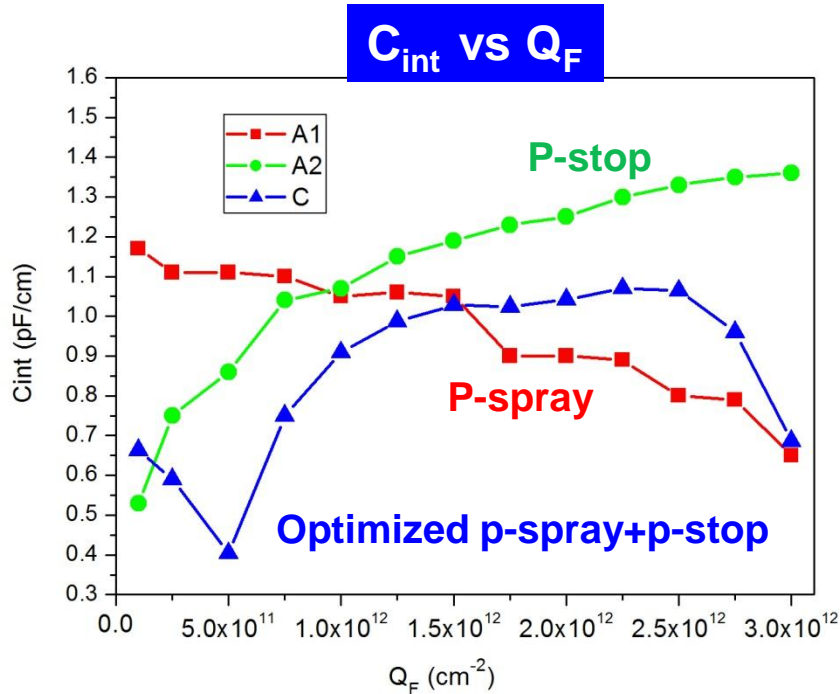
Aim was to optimize these conc. - optimized results are achieved for $N_{pspray} = 4 \times 10^{16} \text{ cm}^{-3}$ and $N_{pstop} = 1 \times 10^{17} \text{ cm}^{-3}$ (Set C).

Set C is able to preserve isolation for all values of Q_F .





Set C: P-spray + P-stop

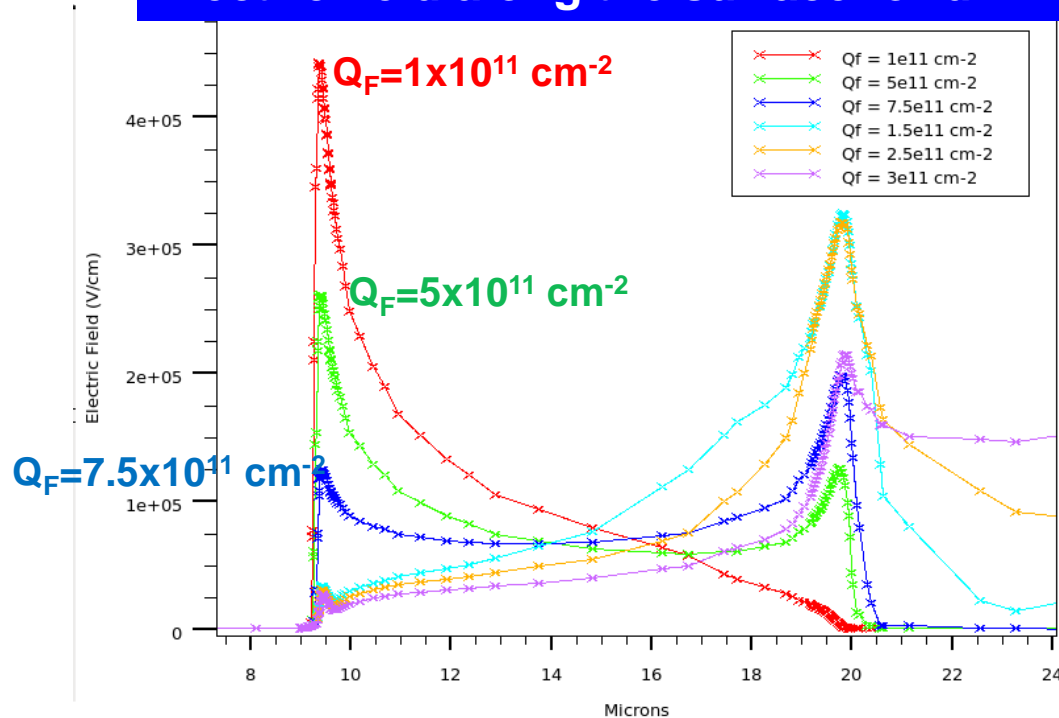


- For $Q_F = 1 \times 10^{11} \text{cm}^{-2}$, C_{int} and V_{BD} fall in between the two extremes of A1 and A2.
- An initial increase in Q_F results in a behaviour similar to that of p-spray (A1)
- However, for $Q_F = 5 \times 10^{11} \text{cm}^{-2}$, the effect of p-spray starts getting neutralized and then p-stop (A2) guides the behaviour of C_{int} and V_{BD} .
- For sufficiently high values of Q_F , i.e. after $Q_F \sim 2 \times 10^{12} \text{cm}^{-2}$, the p-stop also starts getting compensated. But, the structure is still able to support good isolation while improving the breakdown and capacitance performance.



Set C: P-spray + Pstop

Electric field along the surface for diff. Q_F

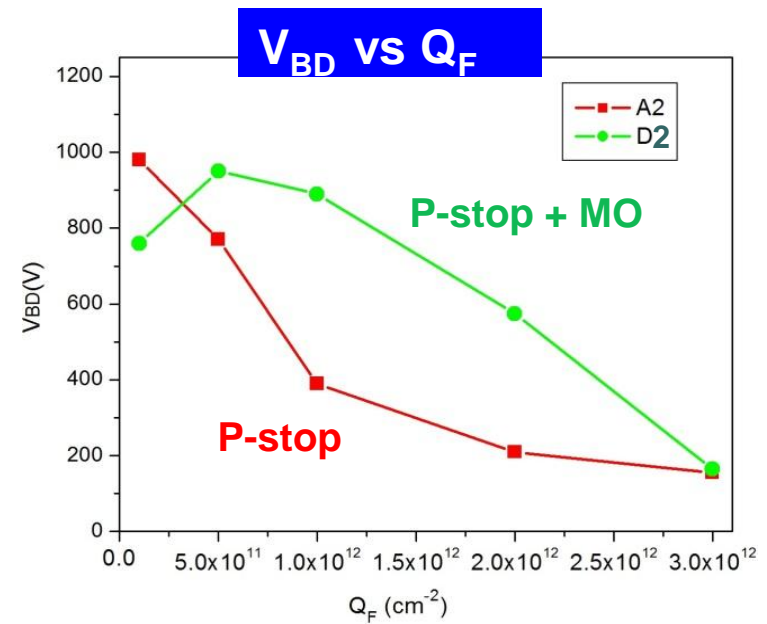
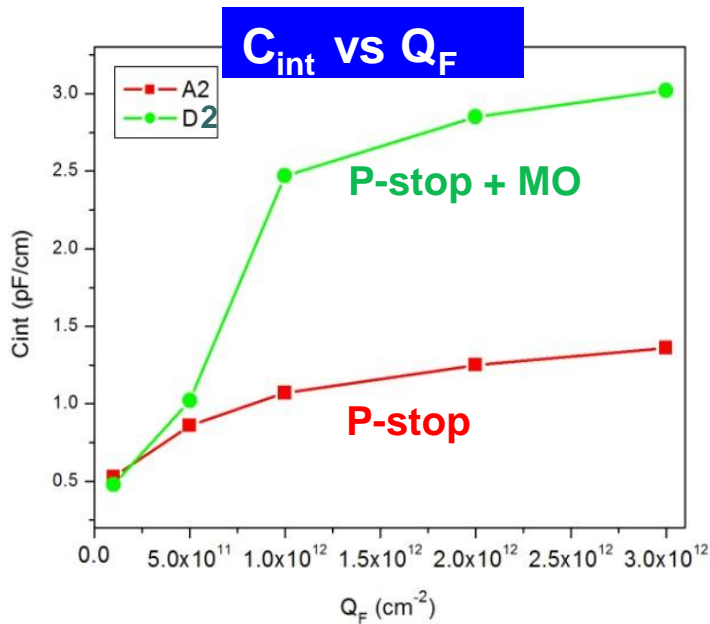


- ❑ For small values of Q_F , the breakdown takes place at the p-spray-n⁺ junction, i.e. when p-spray guides the results.
- ❑ An increase in Q_F results in a shift of peak electric field from p-spray-n⁺ junction to the curvature of p-stop, p⁺-n⁻ junction.
- ❑ For very large values of Q_F peak electric field starts reducing at the p-stop junction and becomes higher all along the surface.



Set D: P-stop+ MO

- ❑ Structure D1 defines a metal overhang of length $5\mu\text{m}$ over n^+ (with p-spray) with SiO_2 thickness below metal overhang equal to $0.2\mu\text{m}$.
- ❑ Structure D2 defines a metal overhang of length $5\mu\text{m}$ over p-stop with SiO_2 thickness below metal overhang equal to $0.5\mu\text{m}$.



- ❑ The use of metal overhang is able to increase the V_{BD} , however, deteriorates the C_{int}



Summary (1)

- ❑ P-stop/p-spray are commonly used tech. to ensure isolation of Si sensors, but, none of these techniques provide optimized electrical characteristics for p⁺-n⁻-n⁺ sensors separately.
- ❑ Investigated the sensors equipped with other possible strategies which include multiple p-stops isolation, p-spray & p-stop combined isolation and use of metal overhang over p-spray/p-stop.
- ❑ Multiple p-stops isolation improve C_{int} as well as V_{BD} without degrading G_{int} .
- ❑ Combined isolation is best among all the techniques investigated for all scenarios of surface damage provided doses are optimized.
- ❑ Use of MO over p-stop to improve V_{BD} is not an attractive option as it contributes significantly to C_{int} .

(thanks to IUSSTF for financial assistance)



RD50 Simulation Activity – First Task

from Vladimir Eremin

The set of parameters for cross-test of modeling software:

Detector thickness ----- $d=0.03$ cm

Concentration of shallow donors (phosphorus) ----- $N_{SD} = 6 \times 10^{11}$ cm⁻³

Bulk generated current calculated from

- Single level model
- Effective energy of current generating level ----- $E_j = 0.65$ eV
- Effective cross-section of current generating level ----- $\sigma_j = 1 \times 10^{-13}$ cm²
- Introduction rate of current generating level ----- $G_j = 1$ cm⁻¹

Radiation induced deep levels

Type of defect	Activation energy, eV	Trapping cross section, cm ²	Introduction rate, cm ⁻¹
Deep donor	$E_{DD} - E_V = 0.48$	$\sigma_e = \sigma_h = 1 \times 10^{-15}$	$G_{DD} = 1$
Deep acceptor	$E_{DA} - E_V = 0.595$	$\sigma_e = \sigma_h = 1 \times 10^{-15}$	$G_{DA} = 1$

We will compare the results of simulation for the following set of parameters:

$T = 290$ K and 260 K

← **TEMP. variation**

$V = 200$ V, 300 V, 500 V, 1000 V at $F = 1 \times 10^{15}$ cm⁻²

← **BIAS variation**

$F = 1 \times 10^{13}$, 1×10^{14} , 3×10^{14} , 1×10^{15} , 3×10^{15} cm⁻² at $V = 300$ V

← **FLUENCE variation**

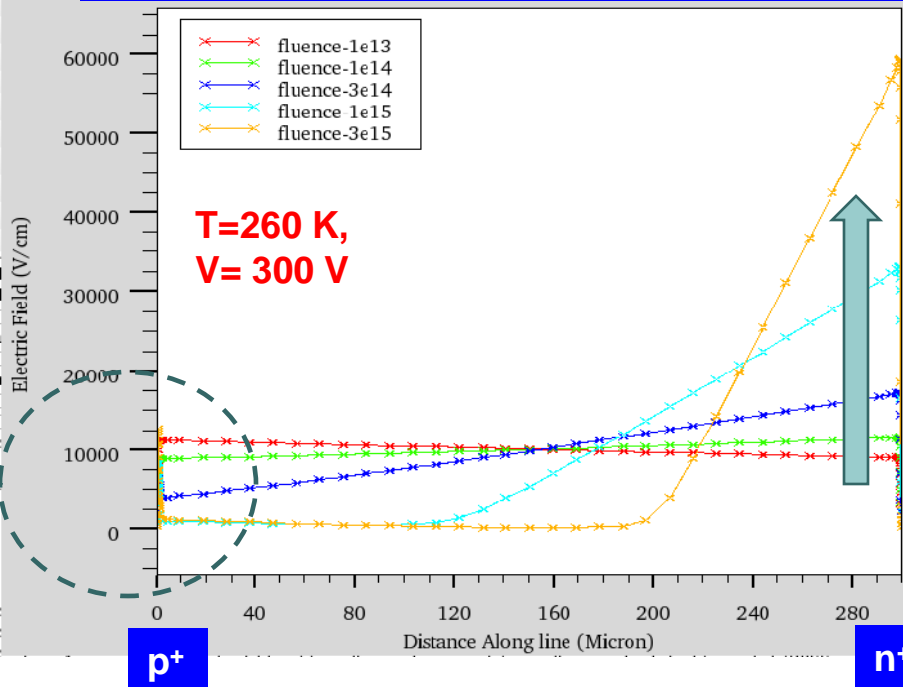
Device structure: Plane parallel 2-D, p⁺-n⁻-n⁺ diode, with 100μm width & 300 μm depth
1-D electric field is seen at the middle of the diode (i.e. at 50μm) along the device depth.



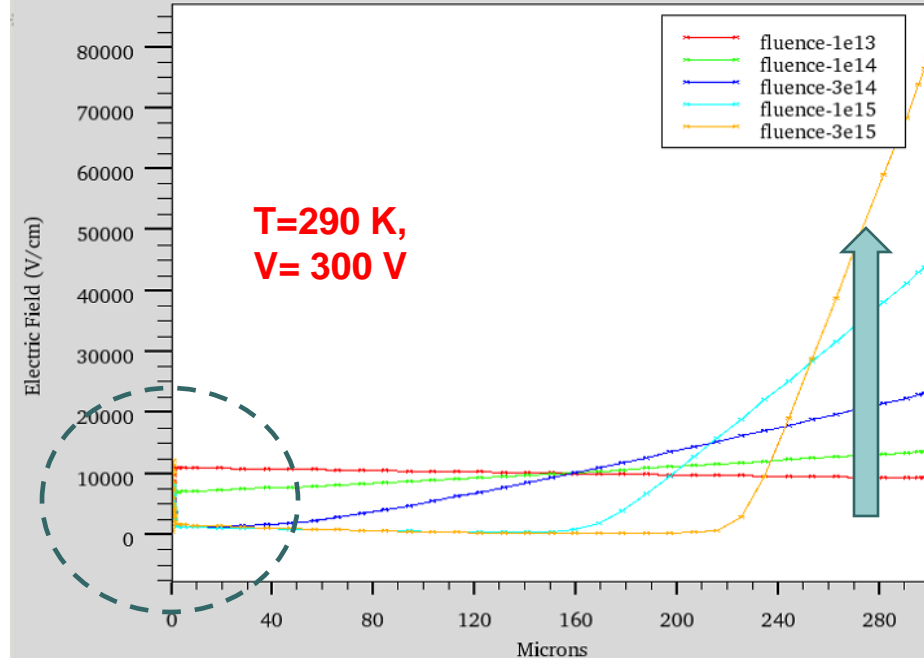
RD50 Simulation Activity – First Task

- Since ATLAS (Silvaco) doesn't have a way of incorporating “Bulk Generation Current level” so the first results were obtained without it.

Electric field along the depth for diff. fluence



Electric field along the depth for diff. fluence



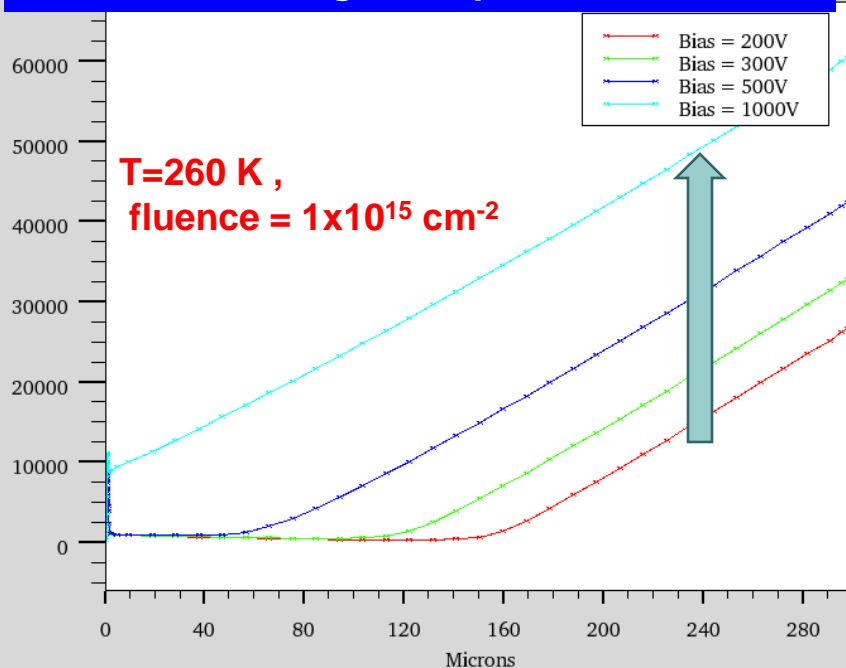
- Temperature & Fluence dependence
- In the absence of bulk current level => double peak structure is rather suppressed.



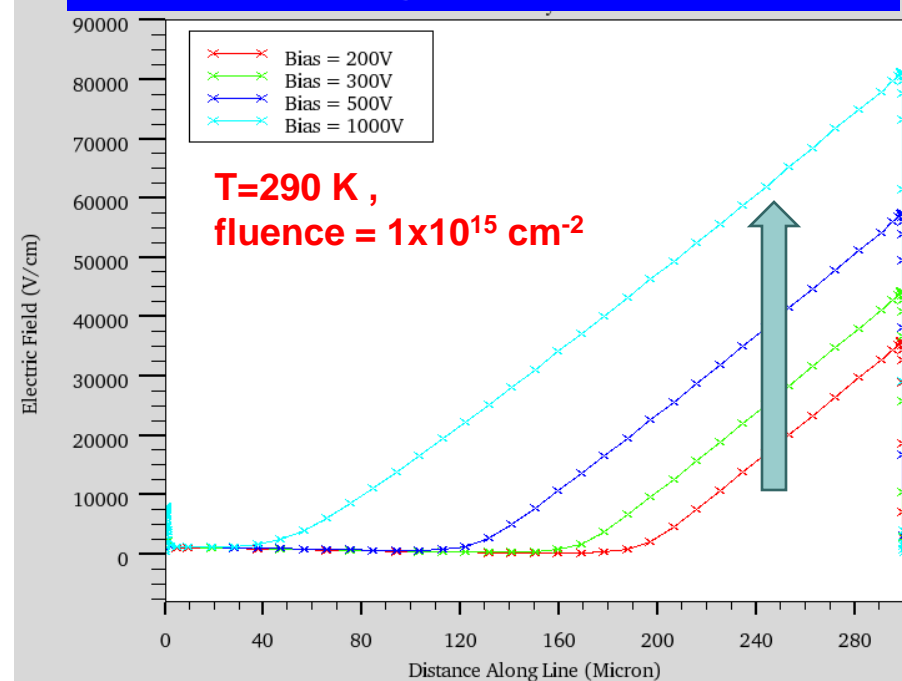
RD50 Simulation Activity – First Task

- No “Bulk Generation Current level”

Electric field along the depth for diff. bias



Electric field along the depth for diff. bias



- ❑ Temperature & Bias dependence
- ❑ In the absence of bulk current level => double peak structure is rather suppressed.



RD50 Simulation Activity – First Task

- To increase current, two possibilities exist:
 - Change Carrier Life-times
 - Change Capture Cross-sections of electron and hole
 - (*"Simulation of Heavily Irradiated Silicon Pixel Sensors and Comparison With Test Beam Measurements"*, by V. Chiochia et al., *IEEE Trans. Nucl. Sci.*, Vol. 52, No. 4, Aug.2005) - ISE TCAD package, Integrated System Engineering AG, Zurich, Swiss.
 - “It is possible to implement the EVL model in TCAD simply **by setting and by varying the size of the common cross section** until the generation current is equal to the observed or expected leakage current.
 - The trap occupancies are not affected in zeroth order by the rescaling, but the leakage current and the free carrier densities are affected by it.
 - The carrier densities have a first-order effect on the occupancies so that varying does alter the effective carrier density.
 - This approach uses the same trapping states to produce space charge and leakage current
- “It is not necessary to introduce current-generating states”***

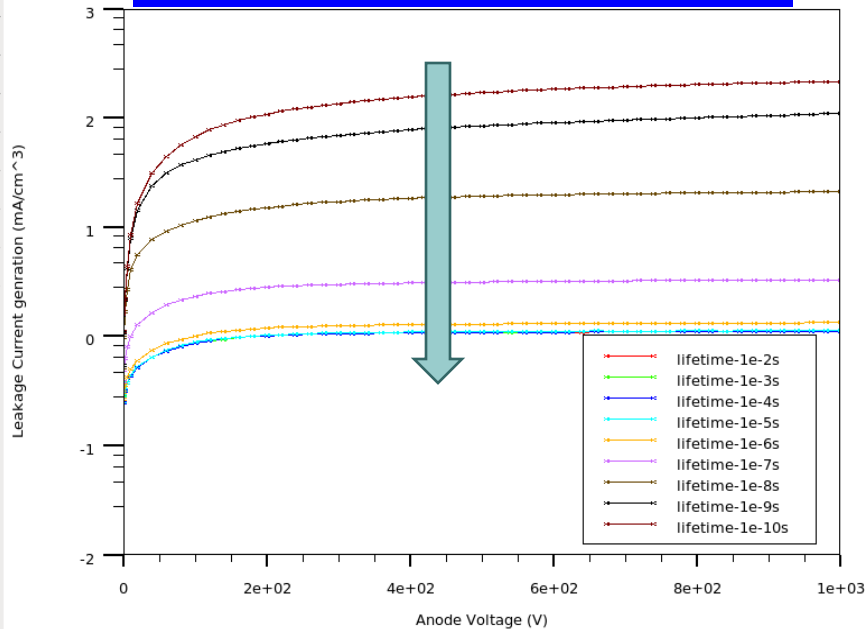


RD50 Simulation Activity – First Task

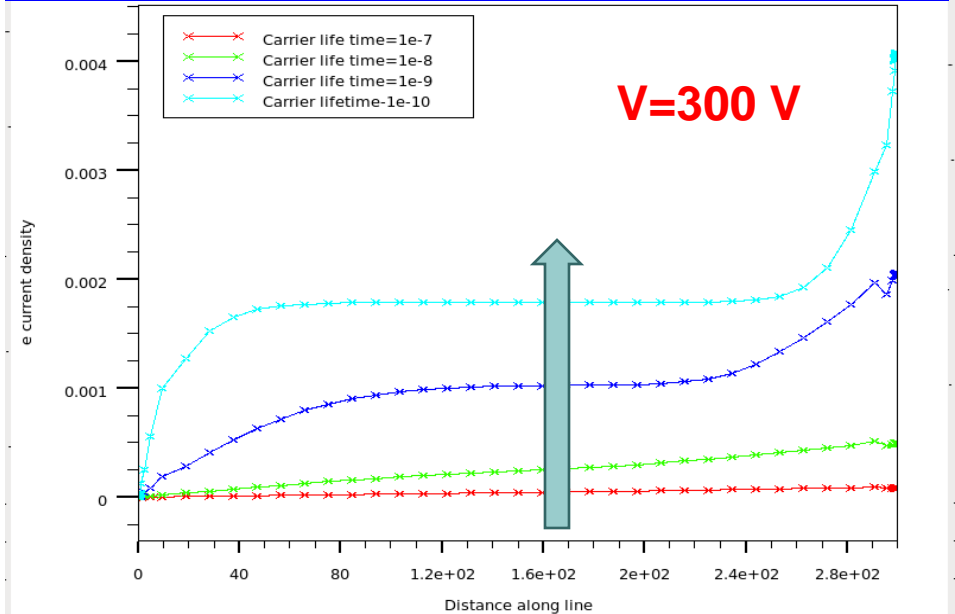
Varying carrier lifetime

$T=290\text{ K}$, fluence = $1 \times 10^{15}\text{ cm}^{-2}$

Current vs. Bias for diff. lifetime



e- current density along the depth for diff. lifetime

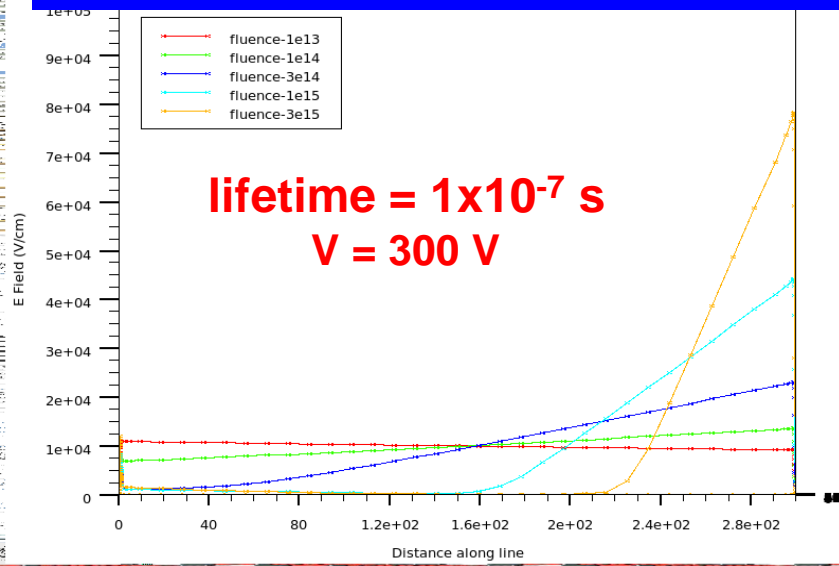


- ❑ **Current decreases as carrier lifetime increases**
- ❑ **Electron current density profile changes with changing carrier lifetime**

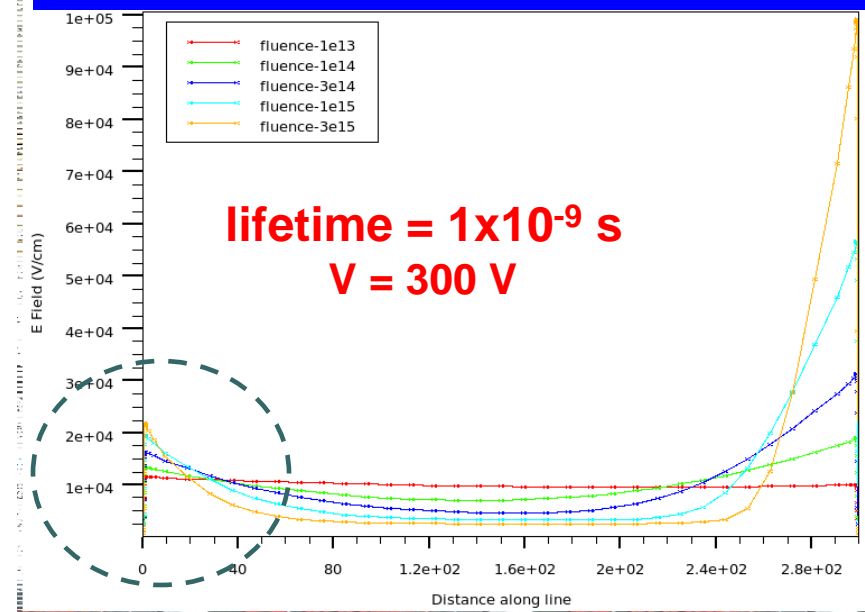


RD50 Simulation Activity – First Task

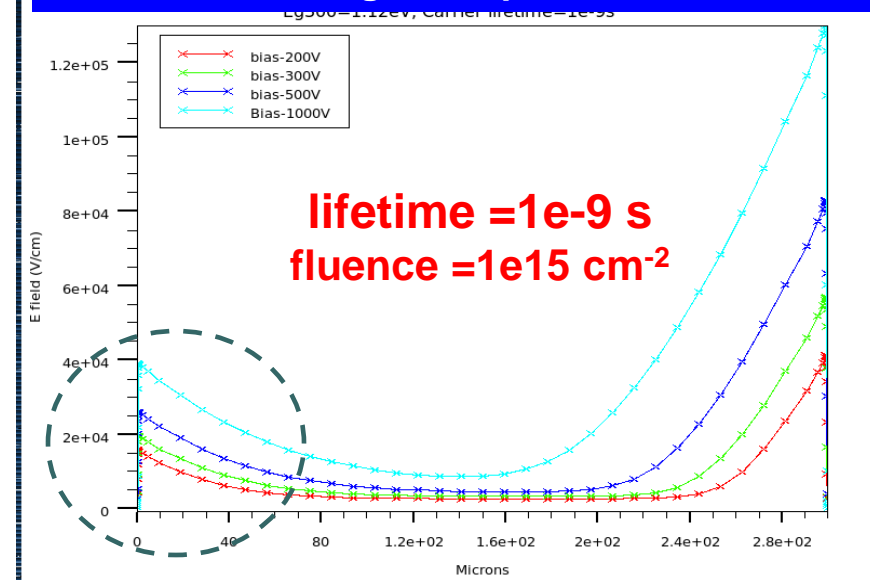
Electric field along the depth for diff. fluence



Electric field along the depth for diff. fluence



Electric field along the depth for diff. bias



- Electric field profile changes with change in lifetime
 \Rightarrow shows signature of double peak for reduced lifetime.



RD50 Simulation Activity – First Task

Varying carrier cross-sections

("Simulation of Heavily Irradiated Silicon Pixel Sensors and Comparison With Test Beam Measurements", by V. Chiochia et al. (IEEE Trans. Nucl. Sci., Vol. 52, No. 4, Aug.2005)

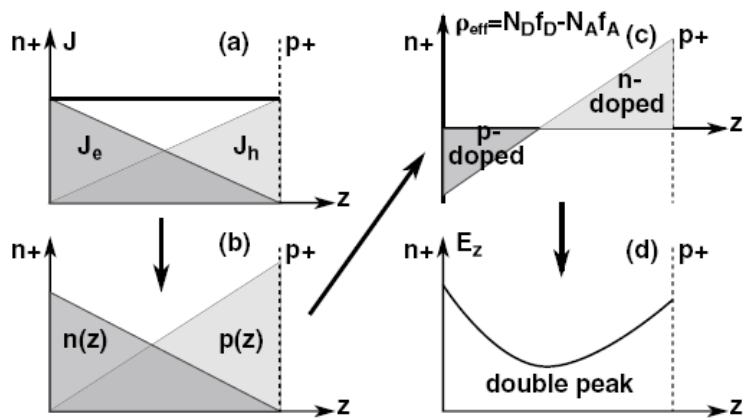


Fig. 6

Position of the charge density minimum can be obtained by decreasing the ratio of hole to electron cross-sections

$$(\sigma_h^D / \sigma_e^D = 0.25 \text{ and } \sigma_h^A / \sigma_e^A = 0.25)$$

“EVL model doesn’t produce sufficiently large electric field on the p+ side”

Change Introduction rate (trap densities/fluence) of carriers to increase the electric field at the p+ side -

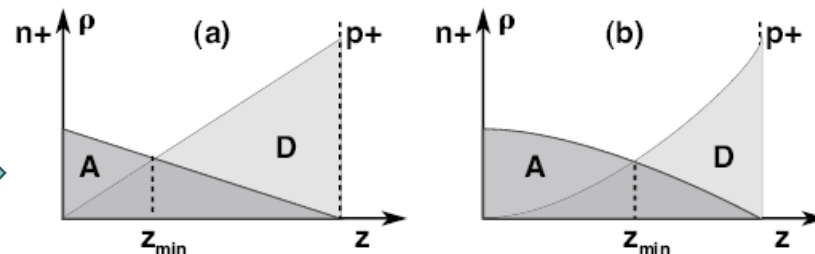


Fig. 8

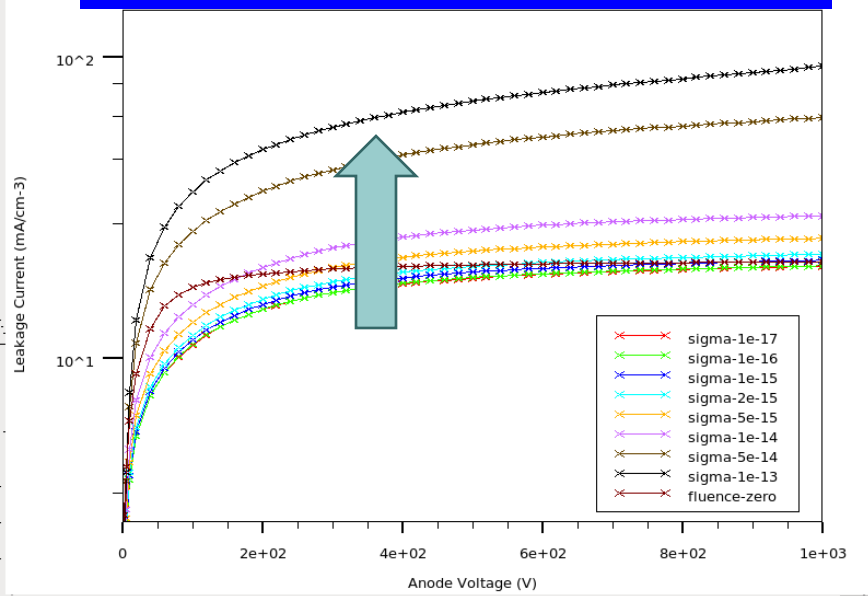
THE EFFECT OF INCREASING N_D/N_A WHEN (A) THE ELECTRON AND HOLE CROSS SECTIONS ARE EQUAL, AND WHEN (B) $\sigma_h/\sigma_e = 0.25$.



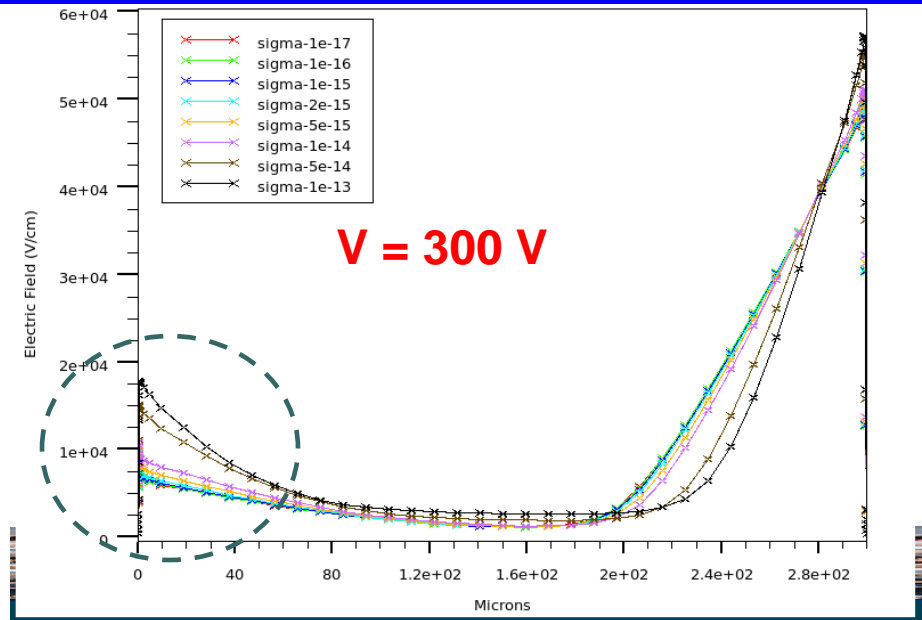
RD50 Simulation Activity – First Task

Varying carrier cross-sections

Current vs. Bias for dff. Cross-sections



Electric field along the depth for dff. Cross-sections



Lifetime = 1×10^{-8} s, fluence = 1×10^{15} cm⁻², T=290 K

- ❑ Current increases with increase in cross-section
- ❑ Electric field profile changes with change in cross-section
 - ❑ shows signature of double peak for large values of cross-section.



Summary(2)

- ❑ **Simulation of the bulk generation current level may be achieved using:**
 - ❑ **carrier lifetime,**
 - ❑ **capture cross-section**
 - ❑ **introduction rate and ratio of hole to electron cross-sections may need to be varied too.**

(thanks to IUSSTF for financial assistance)



Thanks



Radiation Damage

Bulk damage

- ❑ Introduces deep level centers, increasing trapping centers.
 - Higher leakage current, lowering of CCE and change in effective doping conc.
 - Change in the effective doping conc. of the substrate => higher depletion voltage, which requires sensors to be operated at high operational biases to recover CCE => needs higher V_{BD} .

Surface damage

- ❑ Creates charged states in SiO_2 and contribute to Q_F , raising it to higher values and saturating around $2\text{-}3 \times 10^{12} \text{cm}^{-2}$ => sustainable accumulation electron layer under Si-SiO_2 interface, shorting these n^+ -strips and increasing interstrip conductance (G_{int})
- ❑ Increase in Interstrip capacitance (C_{int}), typically the largest contributor to the parasitic capacitance => C_{int} has to be small in order to reduce the total electronic noise.

Performance parameters : G_{int} , C_{int} and V_{BD}